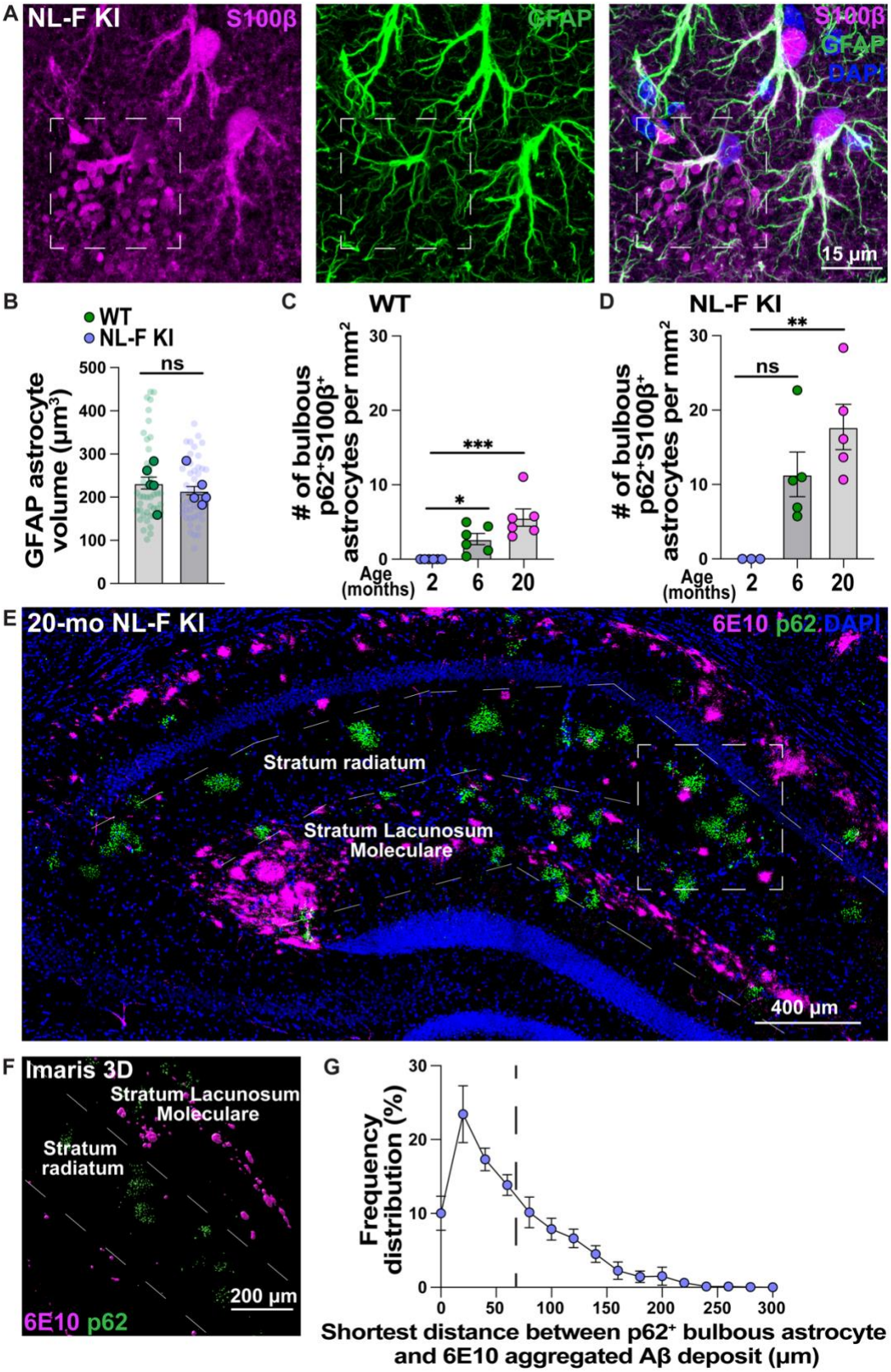

Fig S1. Bulbous astrocytes do not spatially correlate with Aβ plaques. A) Representative image of S100β (magenta) and GFAP (green) immunoreactivity in the hippocampus. Scale bar = 15 μm. Inset highlights exemplar of S100β$^+$ processes that are not labeled by GFAP. **B)** Quantification of the GFAP$^+$ astrocytic volume (μm^3) using Imaris 3D surface rendering. Transparent points = individual astrocytes

(7-11 astrocytes per mouse; 41 WT and 45 NL-F KI astrocytes sampled in total); full points = mouse average of ROIs (n=5 male mice per genotype). Unpaired two-tailed student's t-test on mouse average. **C-D)** Quantification of the number of $p62^+$ $S100\beta^+$ bulbous astrocytes per mm^2 in the WT **(C)** or NL-F KI **(D)** hippocampus. Each point = 1 mouse (n=3-6 male mice per age). Kruskal-Wallis ($p<0.0001$ **(C)** and $p<0.01$ **(D)**) test followed by the Dunn's multiple comparisons test on mouse average. **E)** Representative image of p62 (green) and 6E10 (magenta) immunoreactivity in the 20-mo NL-F KI hippocampus. Scale bar = 400 µm. Dashed square represents ROI zoom for **F**. Dashes lines separated the stratum radiatum and stratum lacunosum moleculare. **F)** Imaris 3D reconstruction of p62-accumulated bulbous astrocytes (green) and 6E10-immunoreactive aggregated Aβ deposits (magenta). Scale bar = 200 µm. **G)** Quantification of shortest distance (µm) between p62-accumulated bulbous astrocytes and 6E10-labeled aggregated Aβ deposits. Data shown as frequency distribution (%) of p62-accumulated bulbous astrocytes (n=5 male mice). Dashed line represents the median distance. All data shown as mean ± SEM. p-values shown ns P>0.05; *P<0.05; **P<0.01; ***P<0.001; ****P<0.0001.

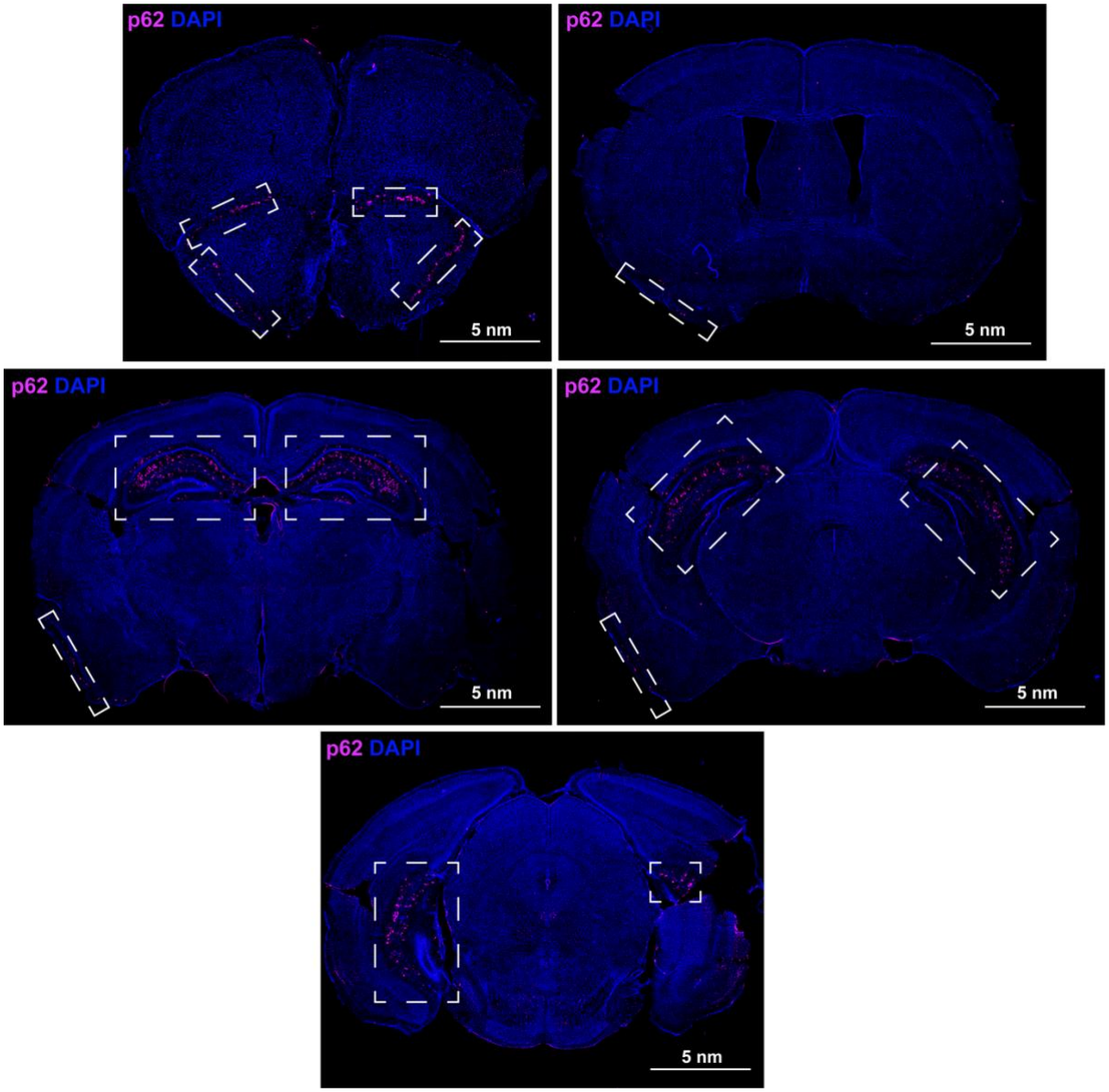

Fig S2. p62-accumulated bulbous astrocytes are found in a region-specific manner in the mouse cerebrum. A) Representative images of p62 (magenta) immunoreactivity in serial brain cross across the cerebrum in a 20-mo NL-F KI mouse. Only regions with bulbous p62-accumulated S100β^{+} astrocytes are represented i.e. piriform cortex, hippocampus and subiculum. Scale bar = 5 nm. Spatial patterning recapitulated in n=6 mixed age/genotype/sex mice. Insets highlight regions where bulbous astrocytes were found.

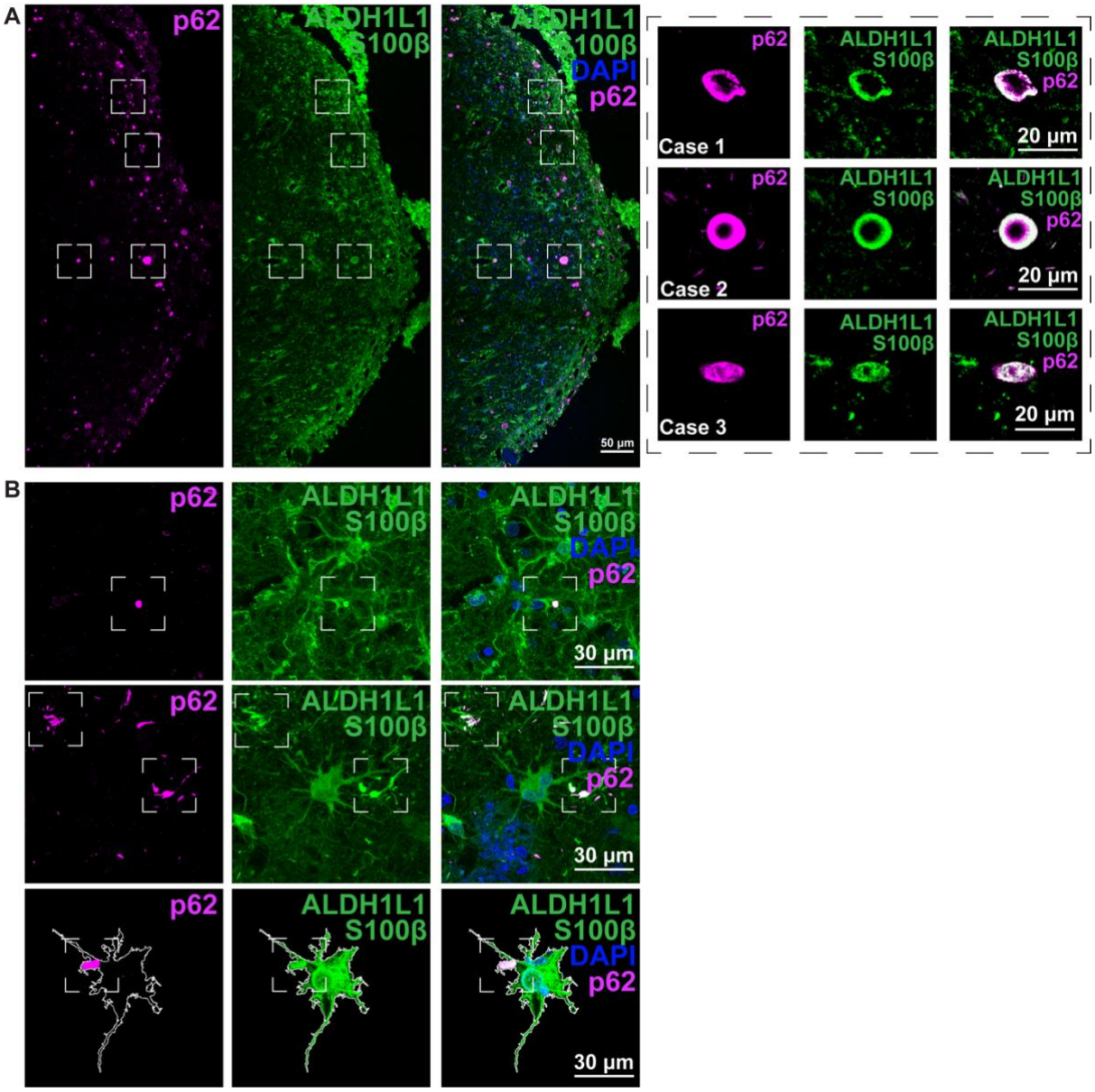

Fig S3. Analogous p62-accumulated astrocyte profile may exist in the human post-mortem hippocampus. A) Representative images of p62 (magenta) and S100β/ALDH1L1^{+} (green) astrocytes in the human hippocampus. Inset highlight representative zoom-ins of three different cases. Scale bar = 50, 20 μm. **B)** Representative images of p62 (magenta) and S100β/ALDH1L1^{+} (green) astrocytes in the human hippocampus. Scale bar = 30 μm. (n=2). Images are modified on ImageJ as shown by white ROI. Insets highlight ROIs. Representative images are shown from both control and AD patients. Please see **Table 1** for patient demographics.

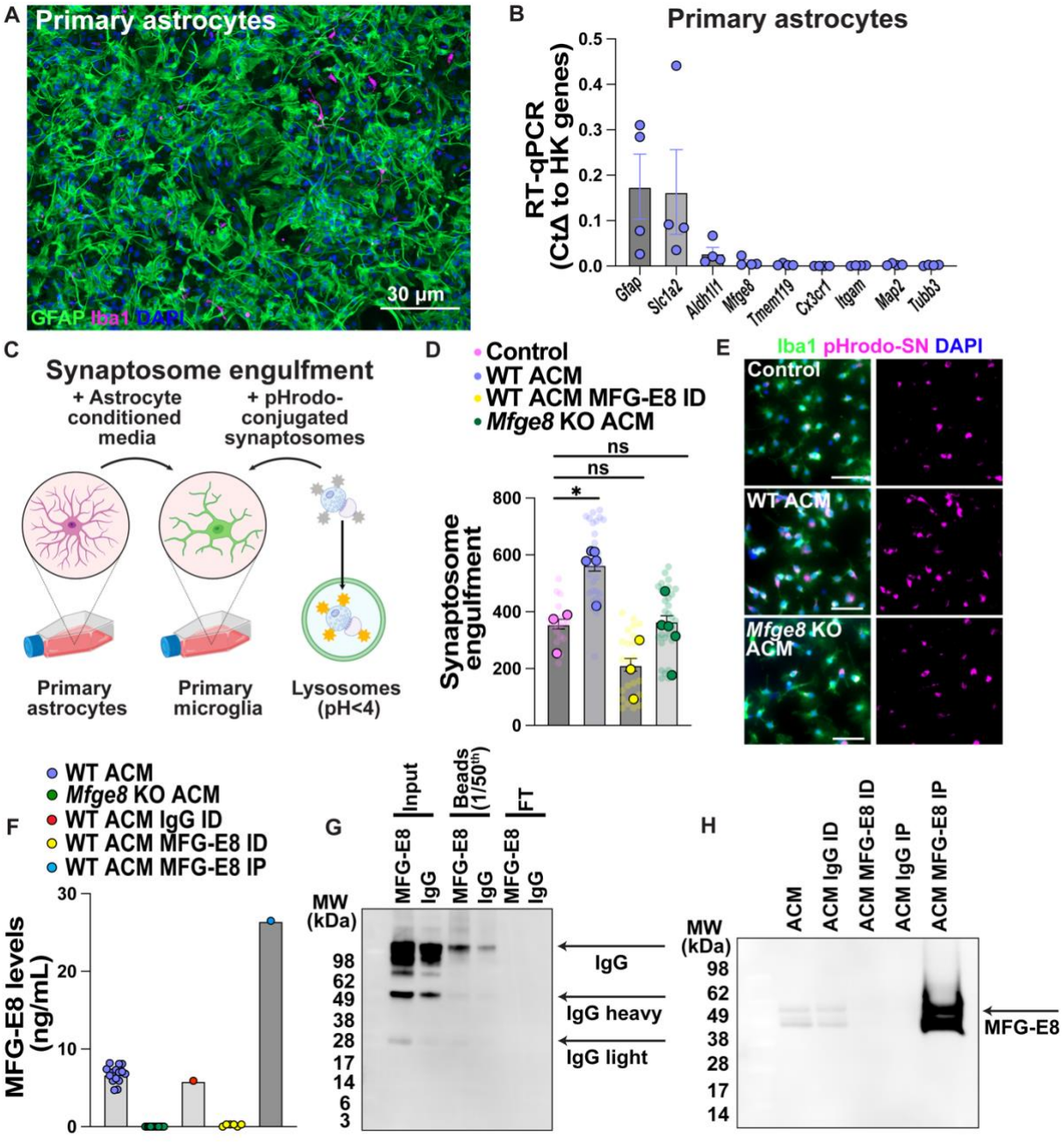

Fig S4. Secreted MFG-E8 in astrocyte conditioned media is sufficient to promote microglia-synaptosome engulfment. A) Representative image of GFAP (green) and Iba1 (magenta) immunoreactivity in primary astrocytic cultures. Scale bar = 30 µm. **B)** RT-qPCR probing for gene expression of *Gfap*, *Slc1a2*, *Aldh1l1*, *Mfge8*, *Tmem119*, *Cx3cr1, Itgam*, *Map2* and *Tubb3* in primary astrocytic cultures. Gene expression is normalized to the geomean of 3 housekeeping genes (*Actb*, *Gapdh* and *Rpl32*) by the Delta CT method. Each point = 1 well (n=4 wells). **C)** Schematic of primary microglial synaptosome engulfment assay using ACM collected from primary astrocytes. **D)** Quantification of the pHrodo fluorescence intensity with time shown as area under curve. Transparent points = individual ROIs with approx. 30 microglia per ROI (2-12 ROIs culture preparation; 17 control microglial media, 28 WT ACM, 29 *Mfge8* KO ACM and 22 WT ACM MFG-E8 ID ROIs sampled in total), full points = culture average of ROIs (n=3-5 mixed male and female culture preparations). One-way

ANOVA followed ($F(3, 12) = 10.86$, $p<0.001$) by Bonferroni's multiple comparisons post-hoc test on culture average. **E)** Representative images of Iba1 (green) immunoreactivity and pHrodo-synaptosomes (SN) (magenta) in primary microglial cultures treated with either control media, WT ACM or *Mfge8* KO ACM using widefield microscopy on the Celldiscoverer 7. Scale bar = 40 µm. **F)** Mouse MFG-E8 ELISA probing for levels of MFG-E8 (ng/mL) in WT ACM, *Mfge8* KO ACM and fractions from the MFG-E8 ID reaction (IgG ID, MFG-E8 ID and MFG-E8 IP). Each point = 1 culture well (15 WT and 15 MFG-E8 KO wells sampled in total across 2-3 independent culture preparations) or ID preparation (6 WT MFG-E8 ID ACM preparations sampled in total, 1 IgG ID and 1 MFG-E8 IP sampled as control). **G)** Western blot probing for goat IgG (150, 50 and 25 kDa) using a secondary anti-goat HRP in the ID reaction. The lanes represent the input antibody put into the reaction, 1/50th of the total beads and the flow through (FT) for MFG-E8 and an IgG control reaction. **H)** Western blot probing for MFG-E8 (55 kDa) in the fractions from the ACM ID reaction (input, IgG ID, MFG-E8 ID, IgG IP and MFG-E8 IP). All data shown as mean ± SEM. p-values shown ns $P>0.05$; *$P<0.05$; **$P<0.01$; ***$P<0.001$; ****$P<0.0001$.

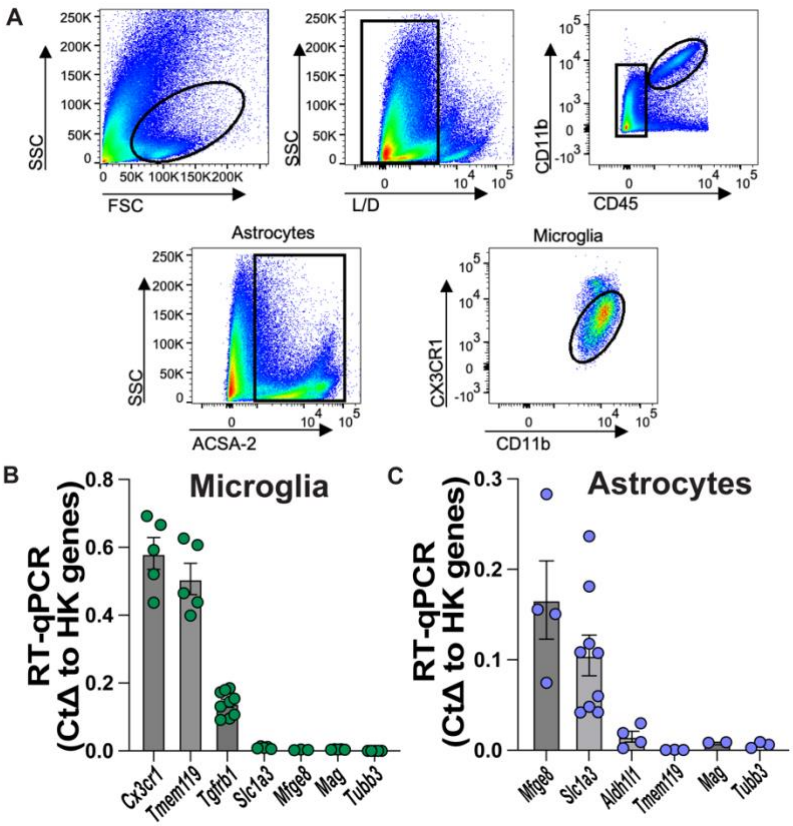

Fig S5. Validation and characterization of FACS cell sorting. A) Flow cytometry plots showing gating strategy based on forward (FSC), side scatter (SSC) and levels of ACSA-2, CD11b, CD45 and CX3CR1. Microglia are selected based on live and CX3CR1^{+}CD45^{+}CD11b^{+}. Astrocytes are selected based on live and ACSA-2^{+}CD45^{-}. **B)** RT-qPCR probing for gene expression of *Cx3cr1*, *Tmem119*, *Tgfrb1*, *Slc1a3*, *Mfge8*, *Mag* and *Tubb3* on FACS sorted CX3CR1^{+}CD45^{+}CD11b^{+} microglia. Gene expression is normalized to the geomean of 3 housekeeping genes (*Actb*, *Gapdh* and *Rpl32*) by the Delta CT method. Each point = 1 mouse (n=3-9 female mice). **C)** RT-qPCR probing for gene expression levels of *Mfge8*, *Slc1a3*, *Aldh1l1*, *Tmem119*, *Mag* and *Tubb3* on FACS sorted ACSA-2^{+}CD45^{-} astrocytes. Gene expression is normalized to the geomean of 3 housekeeping genes (*Actb*, *Gapdh* and *Rpl32*) by the Delta CT method. Each point = 1 mouse (n=2-9 female mice). All data shown as mean ± SEM.

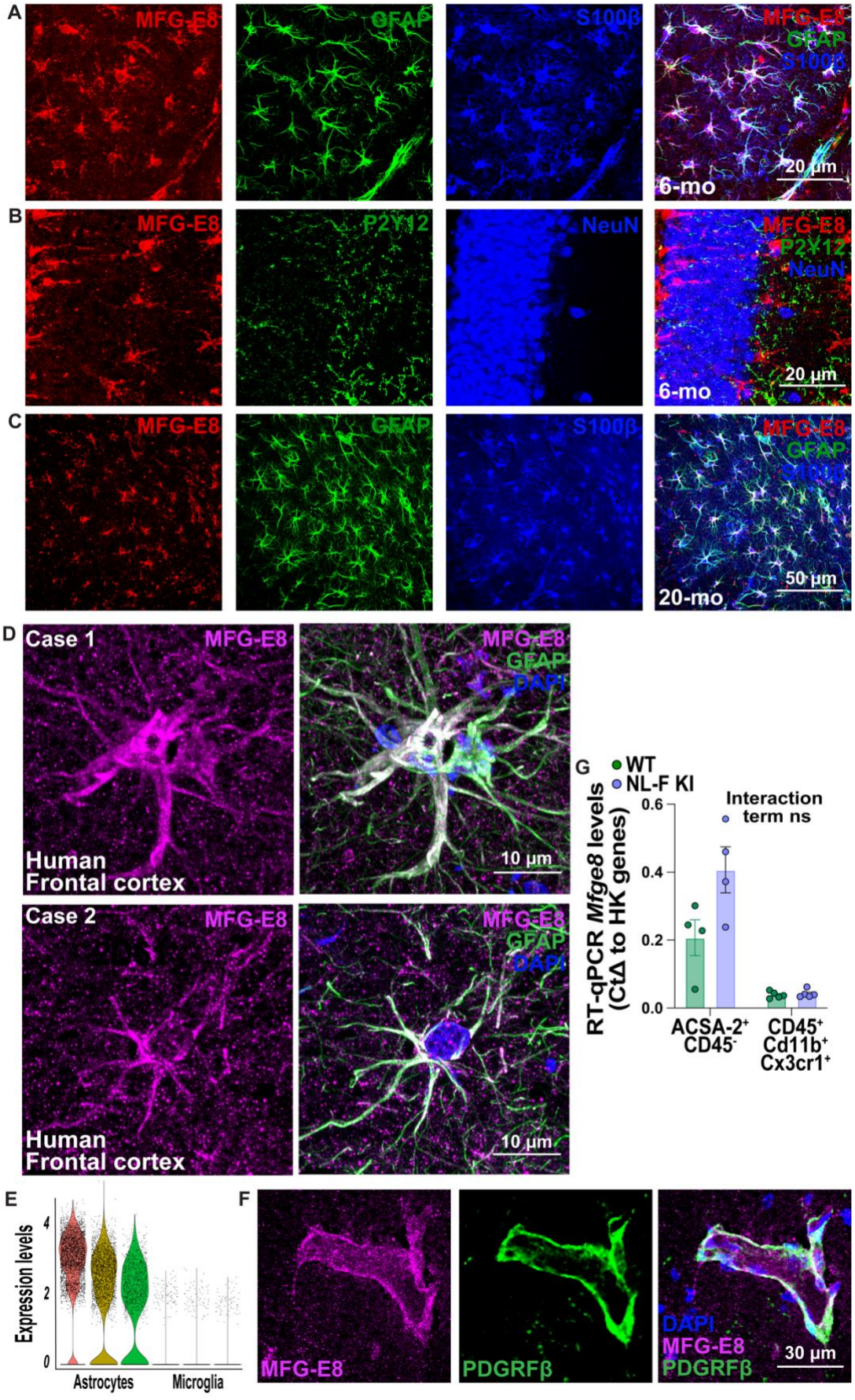

Fig S6. MFG-E8 is expressed by astrocytes in the mouse and human brain parenchyma. A) Representative image of MFG-E8 (red) and GFAP$^+$ (green) and S100β$^+$ (blue) astrocytes in the 6-mo mouse hippocampus. Scale bar = 20 μm. **B)** Representative image of MFG-E8 (red), P2Y12$^+$ microglia (green) and NeuN$^+$ (blue) neurons in the 6-mo mouse hippocampus. Scale bar = 20 μm. **C)** Representative image of MFG-E8 (red) and GFAP$^+$ (green) and S100β$^+$ (blue) astrocytes 20-mo mouse hippocampus. Scale bar = 20 μm. **D)** Representative image of MFG-E8 (magenta) and GFAP (green) immunoreactivity in the post-mortem human frontal cortex. Representative images are from control and AD patients. Please see **Table 1** for patient demographics. Scale bar = 10 μm. **E)** Single cell RNA sequencing data from the Linnarson database[55] comparing *Mfge8* expression levels on astrocyte and microglial clusters. **F)** Representative image of MFG-E8 (magenta) and PDGFRβ$^+$ (green) immunoreactivity in the mouse hippocampus. Scale bar = 30 μm. **G)** RT-qPCR probing for *Mfge8* gene expression in FACS sorted ACSA2$^+$CD45$^-$ astrocytes and CX3CR1$^+$CD45$^+$CD11b$^+$ microglia from 6-mo WT and NL-F KI mice. Gene expression is normalized to the geomean of 3 housekeeping genes (*Actb*, *Gapdh* and *Rpl32*) by the Delta CT method. Each point = 1 mouse (n=4-5 female mice per genotype). Two-way ANOVA (Interaction: $F(1, 14) = 2.956$, ns $p>0.05$) on Y=log(Y) transformed mouse average. All data shown as mean ± SEM. p-values shown ns P>0.05; *P<0.05; **P<0.01; ***P<0.001; ****P<0.0001.

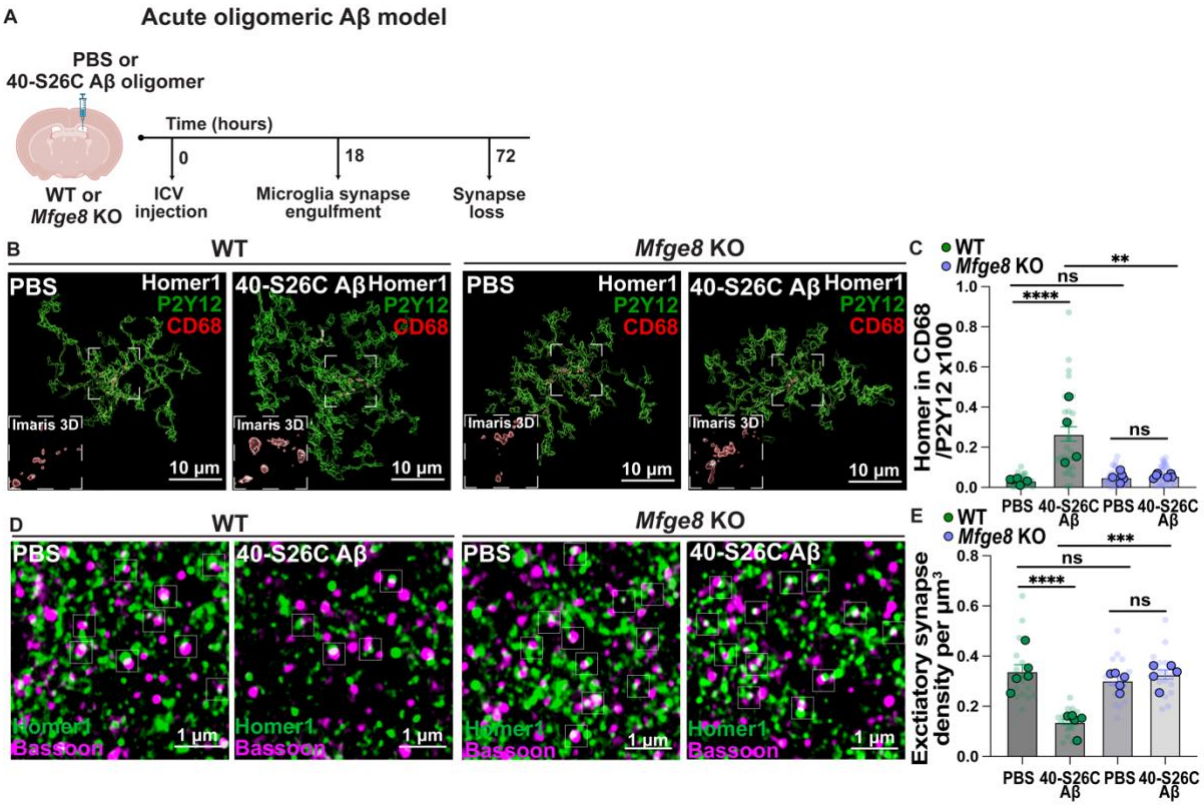

Fig S7. MFG-E8 is necessary for microglia-Homer1 engulfment and excitatory synapse loss in an *in vivo* acute Aβ injection model. A) Schematic of acute 40-S26C oligomeric Aβ ICV injection model. **B)** Representative 3D images for excitatory post-synaptic Homer1 (white), CD68 lysosomes (red) and P2Y12 (green) in the WT or *Mfge8* KO CA1 SR hippocampus post PBS control or synthetic humanized Aβ 40-S26C oligomer ICV injection. Scale bar = 10 µm. Inset shows representative zoom of Homer1 inside $CD68^+$ microglial lysosomes. **C)** Quantification of microglial Homer1 engulfment using Imaris 3D surface rendering shown as: Homer1 volume in $CD68^+$ lysosomes in $P2Y12^+$ microglial surface/P2Y12 volume x100. Transparent points = individual microglia (5-9 microglia per mouse; 33 WT PBS, 28 WT Aβ, 31 *Mfge8* KO PBS and 44 *Mfge8* KO Aβ microglia were sampled in total), full points = mouse average of ROIs (n=4-6 female mice per condition). Two-way ANOVA (Interaction F (1, 16) = 17.39, p<0.001) followed by Bonferroni's multiple comparisons post-hoc test on Y=log(Y) transformed mouse average. **D)** Representative images of excitatory post-synaptic Homer1 (green) and pre-synaptic Bassoon (magenta) immunoreactivity in the WT or *Mfge8* KO SR hippocampus post PBS control or synthetic humanized Aβ 40-S26C oligomer ICV injection using super-resolution Airyscan confocal microscopy. Scale bar = 1 µm. Insets show regions of colocalization. **E)** Quantification of the number of colocalized Homer1 and Bassoon spots shown as density per μm^3 using Imaris. Transparent points = individual ROIs (3 ROIs per mouse; 15 ROIs were sampled per condition in total), full points = mouse average of ROIs (n=5 male mice per condition). Two-way ANOVA (Interaction: F (1, 16) = 23.29, p<0.001) followed by Bonferroni's multiple comparisons post-hoc test on mouse average. All data shown as mean ± SEM. p-values shown ns P>0.05; *P<0.05; **P<0.01; ***P<0.001; ****P<0.0001.

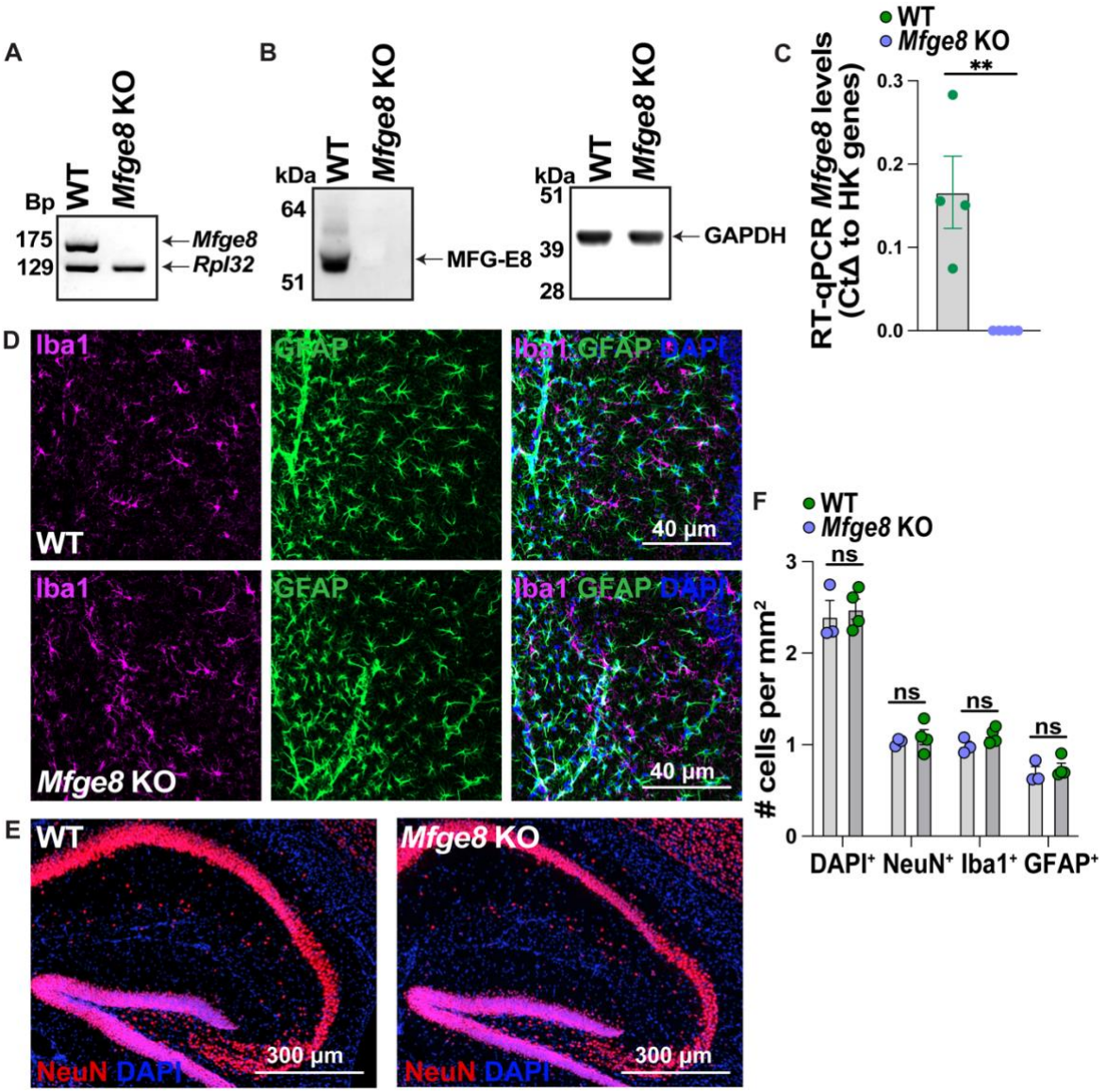

Fig S8. Validation and characterization of the *Mfge8* KO mouse model. A) PCR probing for *Mfge8* expression in hippocampal homogenate resolved on agarose gel with respect to housekeeping gene *Rpl32*. 1 lane = 1 mouse. **B)** Western blot probing for MFG-E8 (55-75 kDa) with respect to GAPDH loading control (39 kDa) in WT and *Mfge8* KO homogenate. 1 lane = 1 mouse. **C)** RT-qPCR probing for *Mfge8* gene expression in FACS sorted ACSA2^{+}CD45^{-} astrocytes from WT and *Mfge8* KO mice. Gene expression is normalized to the geomean of 3 housekeeping genes (*Actb*, *Gapdh* and *Rpl32*) by the Delta CT method. Each point = 1 mouse (n=4-5 female mice per genotype). Mann-Whitney test on mouse average. **D)** Representative images of GFAP (green) and Iba1 (magenta) immunostaining in the hippocampus of WT and *Mfge8* KO mice. Scale bar = 40 µm. **E)** Representative images of NeuN (red) immunoreactivity in the hippocampus of WT and *Mfge8* KO mice. Scale bar = 300 µm. **F)** Quantification of the number of total DAPI^{+} cells, GFAP^{+} astrocytes, Iba1^{+} microglia and NeuN^{+} neurons in the hippocampus shown as number per mm^{2} using Imaris 3D surface rendering. Each point = 1 mouse (n=3-4 female mice per genotype). Multiple unpaired t-tests followed by Dunn's multiple comparisons correction on mouse average. All data shown as mean ± SEM. p-values shown ns P>0.05; *P<0.05; **P<0.01; ***P<0.001; ****P<0.0001.

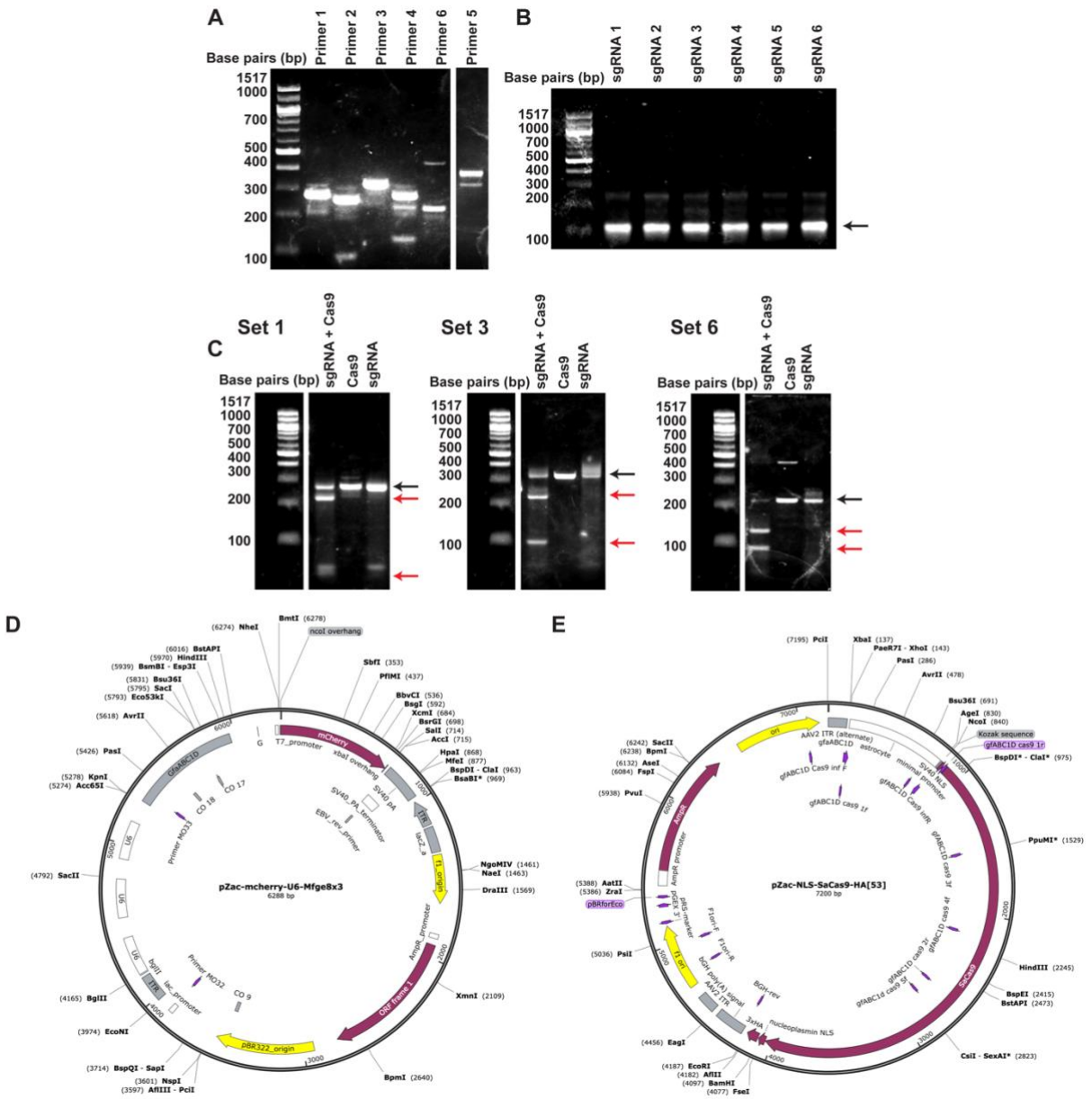

Fig S9. Design and testing of CRISPR-saCas9 paradigm. A) PCR product resolved on agarose gel after amplification of genomic DNA (gDNA) regions of the *Mfge8* gene. These gDNA amplicons correspond to the cleavage regions of the sgRNAs. Primer 1-6 refers to the primer set used to amplify each region. Expected amplicon product lengths: primer 1, 275 bp; primer 2, 254 bp; primer 3, 323 bp; primer 4, 275 bp; primer 5, 380 bp; primer 6, 232 bp. **B)** PCR product resolved on agarose gel after amplification of 6 DNA templates for subsequent transcription of the sgRNA molecules. Each template corresponds to one sgRNA sequence. The arrow points at the expected amplicon length (121 bp). **C)** *In vitro* digestion assay resolved on agarose gel to assess the cleavage efficiency of each designed sgRNA. The reaction was performed with the sgRNA + Cas9 or as a control the Cas9 or sgRNA alone. Black arrows indicate the input gDNA length and the red arrows indicate the expected cleavage fragments. Only the three successful reactions are shown here. Expected fragment lengths: Set 1, 218 bp and 31 bp; Set 3, 206 bp and 90 bp, Set 6, 127 bp and 104 bp. **D)** *Mfge8*gRNA-*GfaABC$_1$D*-mCherry plasmid construct map. **E)** *GfaABC$_1$D*-saCas9-HA plasmid construct map.

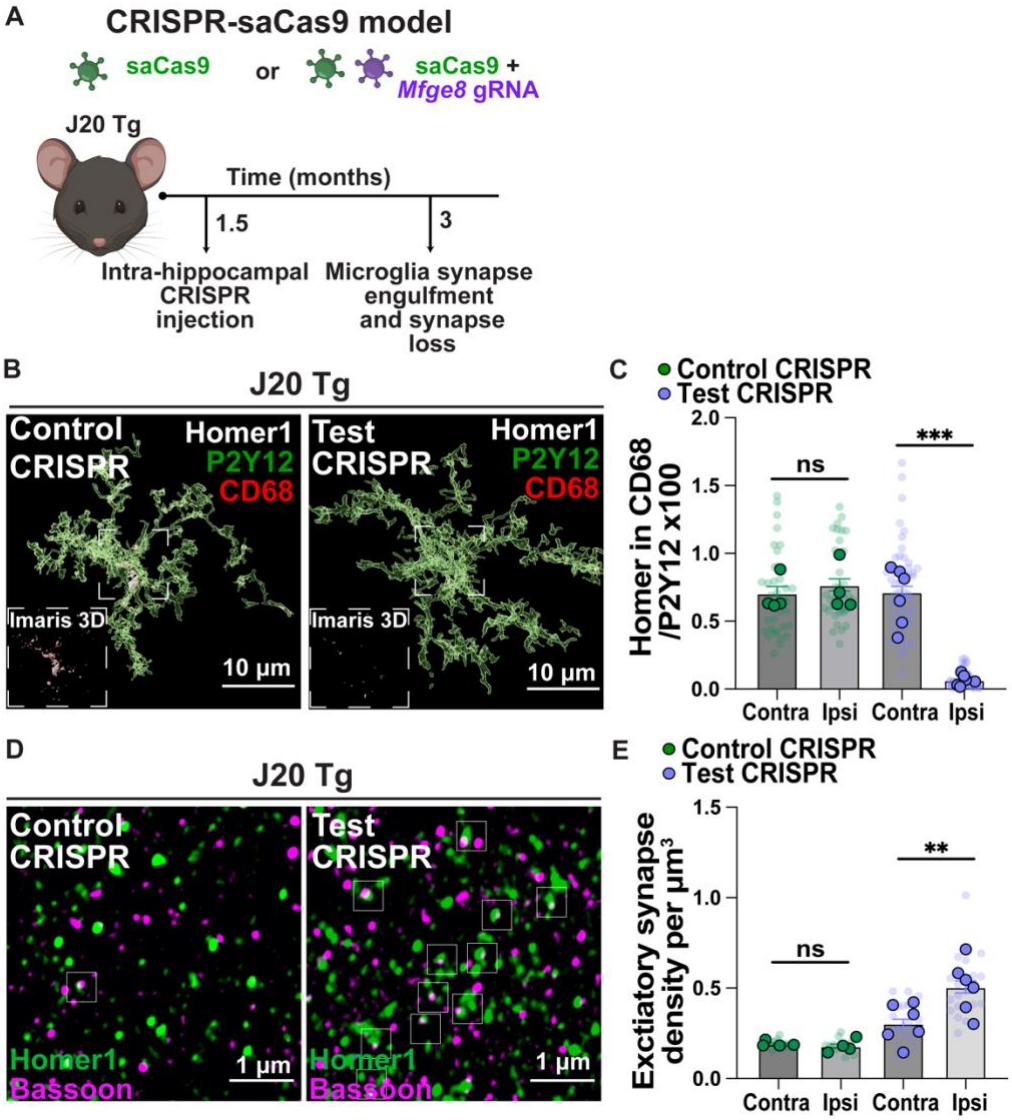

Fig S10. Preventative viral CRISPR-saCas9 deletion of astrocytic MFG-E8 rescues microglia-Homer1 engulfment and excitatory synapse loss in a second model of amyloidosis, the J20 Tg. **A)** Schematic of CRISPR-saCas paradigm to knock-down *Mfge8* from hippocampal astrocytes with spatio-temporal control. **B)** Representative 3D images for excitatory post-synaptic Homer1 (white), CD68 lysosomes (red) and P2Y12 (green) in the 3mo J20 Tg CA1 SR hippocampus post control or test CRISPR-saCas9 injection. Scale bar = 10 µm. Inset shows representative zoom of Homer1 inside CD68$^+$ microglial lysosomes. **C)** Quantification of microglial Homer1 engulfment using Imaris 3D surface rendering shown as: Homer1 volume in CD68$^+$ lysosomes in P2Y12$^+$ microglial surface/P2Y12 volume x100. Transparent points = individual microglia (6-11 microglia per condition; 34 contra control CRISPR, 34 ipsi control CRISPR, 51 contra test CRISPR and 46 ipsi test CRISPR injected microglia were sampled in total), full points = mouse average of ROIs (n=4-6 mixed male and female mice per condition). Multiple paired t-tests followed by the Bonferroni-Dunn correction on mouse average. **D)** Representative images of excitatory post-synaptic Homer1 (green) and pre-synaptic Bassoon (magenta) immunoreactivity in the 3mo J20 Tg CA1 SR hippocampus post control or test CRISPR-saCas9 injection using super-resolution Airyscan confocal microscopy. Scale bar = 1 µm. Insets show regions of colocalization. **E)** Quantification of the number of colocalized Homer1 and Bassoon spots

shown as density per μm^3 using Imaris. Transparent points = individual ROIs (3 ROIs per condition; 12 contra control CRISPR, 12 ipsi control CRISPR, 18 contra test CRISPR and 18 ipsi test CRISPR injected ROIs were sampled in total), full points = mouse average of ROIs (n=4-6 mixed male and female mice per condition). Multiple paired t-tests followed by the Bonferroni-Dunn correction on mouse average. All data shown as mean ± SEM. p-values shown ns P>0.05; *P<0.05; **P<0.01; ***P<0.001; ****P<0.0001.